Implementation and comparison of different turbulence models for three dimensional wall jets with FLUENT

Ch. Heschl[1], W. Sanz[2] and P. Klanatsky[1]

Fachhochschulstudiengänge Burgenland GmbH [1]

Steinamangerstraße 21, A-7423 Pinkafeld

TU Graz, Institute for Thermal Turbomachinery and Machine Dynamics [2]

Inffeldgasse 25, A-8010 Graz

Abstract

This paper discusses the capability of different turbulence closure models to predict the remarkable lateral spreading rate of three dimensional wall jets. Based on the equation for the mean streamwise vorticity it can be shown, that the strong lateral spreading rate clearly depends on the anisotropy of the turbulent normal stresses. Therefore it can be that linear eddy viscosity turbulence models are not able to predict the lateral spreading rate of three dimensional wall jets accurately. If Reynolds stress models are used, it can be also derived that the computed results are very sensitive to the chosen pressure strain models. Motivated from this theoretical observation different nonlinear eddy viscosity, pressure strain and hybrid Reynolds stress models were implemented into FLUENT using User Defined Scalars and Functions and computational results are compared with experimental data.

Key Words:

v2f turbulence model, nonlinear v2f turbulence model, cubic pressure strain model, wall reflection effect, two component closure, TCL, hybrid RSM turbulence model, three-dimensional wall jet, UDF

Introduction

The behaviour of 3D turbulent wall jets are very interesting in many technical applications. Especially the film cooling of turbine blades, ceiling diffuser flows and the defrosting of vehicle windscreens represent flow situations in which the velocity distributions are clearly affected by the spreading mechanism of 3D turbulent wall jets.

Several authors have discussed the remarkable spreading behaviour of 3D wall jets (e.g. Abrahamsson 1997, Launder and Rodi 1983 and Newman et al. 1972). Craft and Launder (2001) reported on a detailed computational investigation which aimed to identify the origin of the large lateral spreading mechanism. It was concluded, that the high lateral rate of spread can be attributed to stress-induced axial vorticity, which is generated by the anisotropy of the Reynolds normal stresses perpendicular to the jet axis (cp. Lübcke et al. 2003). The correct prediction of the remarkable lateral spreading rate of a three dimensional wall jet assumes that the Reynolds normal stresses must be modeled realistic.

One way to model the anisotropy is to use the Reynolds stress transport equations. Craft and Launder (2001) discussed different Reynolds stress turbulence models and find out that higher order pressure strain models which consider the stress redistribution near walls can predict the lateral spreading rate well. The good agreement with experimental data is paid however through a high computational effort.

In contrast to Craft and Launder (2001), Lübcke et al. (2003) present an explicit Reynolds-stress closure along a route suggested by Gatski and Speziale (1993), which offers a physically sound extension of the most prominent linear Boussinesq-viscosity models with modest computational effort. Also a promising explicit Reynoldsstress closure is presented by Pettersson Reif (1999). This model is based on the equilibrium solution of second-moment closure for 2D incompressible flow according to Pope (1975). Another promising model is the nonlinear v2f turbulence model which differs from the family of conventional nonlinear eddy viscosity models. Two additional transport equations are solved to determine the wall normal Reynolds stress component $\overline{v'^2}$, which represent the turbulent velocity scale $v = \sqrt{\overline{v'^2}}$. In conjunction with an explicit Reynolds stress closure two advantages can be derived. First a low Reynolds number extension (empirical wall treatment) is not necessary and second the scalar $\overline{v'^2}$ can be used to calibrate the model coefficients to ensure the internal consistent.[1]

In this paper the quality of the spreading rate prediction from a 3D wall jet is discussed. Especially the influence of the anisotropic behaviour in the near wall region of different first and second moment closure turbulence models will be compared.

Used turbulence models

The present study is based on the Reynolds-averaged Navier Stokes (RANS) equation for incompressible fluids and isothermal flows. The continuity and the momentum equation use the following form:

$$\frac{\partial u_j}{\partial x_j} = 0 \qquad (1)$$

[1] The wall normal Reynolds stress component in parallel shear flow should be equal to the scalar $\overline{v'^2}$.

$$\frac{\partial u_i}{\partial t} + \overline{u}_j \frac{\partial u_i}{\partial x_j} = -\frac{1}{\rho}\frac{\partial p}{\partial x_i} + \frac{\partial}{\partial x_j}\left[\nu \frac{\partial u_i}{\partial x_j}\right] - \frac{\partial \overline{u_i' u_j'}}{\partial x_j} \qquad (2)$$

To close the RANS equation the Reynolds stresses $-\rho\overline{u_i' u_j'}$ - which represent the turbulence effects - must be modelled. There are different ways to model these turbulent quantities. One way is based on the eddy viscosity concept and the other uses the differential transport equations for every Reynolds stresses. In this paper a wide range of both concepts are used to determine the spreading rate of three dimensional wall jets. In Table 1 an overview of the used turbulence models are presented.

Table 1: Overview of the used turbulence models

turbulence model designation	*short cut*	*remark*
Standard $k-\varepsilon$ model	ske	standard model in Fluent
$k-\varepsilon$ model with enhanced wall treatment	ske-et	standard model in Fluent
Reynolds stress model with linear pressure strain model and wall reflection term	IP	standard model in Fluent
Reynolds stress model with linear pressure strain model, wall reflection term and enhanced wall treatment	IP-et	standard model in Fluent
Reynolds stress model with quadratic pressure strain model	SSG	standard model in Fluent
v2f model	v2f	in Fluent implemented via UDF
v2f model modified by Davidson	v2f-dav	in Fluent implemented via UDF
nonlinear v2f model by Pettersson Reif (1999)	v2f-pet	in Fluent implemented via UDF
nonlinear v2f model by Pettersson Reif (1999), the v2f turbulence is modified by Davidson	v2f-pede	in Fluent implemented via UDF
nonlinear $k-\varepsilon$ model by Ehrhard (1999)	ske-ehr	in Fluent implemented via UDF
nonlinear $k-\varepsilon$ model by Lübcke (2003)	ske-lue	in Fluent implemented via UDF
Reynolds stress model with cubic pressure strain model	CUBIC	in Fluent implemented via UDF
Reynolds stress model with two component closure pressure strain model	TCL	in Fluent implemented via UDF
Reynolds stress model with linear pressure strain model, standard wall function and wall reflection effect model according to equation (36)	IP-cl	in Fluent implemented via UDF
Hybrid Reynolds stress model with linear pressure strain model and wall reflection term	IP-hyb	in Fluent implemented via UDF
Hybrid Reynolds stress model with quadratic pressure strain model	SSG-hyb	in Fluent implemented via UDF

The first five turbulence models are standard models in Fluent and the other twelve models were implemented via compiled user defined functions (UDF).

Linear eddy viscosity concept

According to the kinetic theory of gases, the molecular viscosity of a fluid is proportional to the product of the molecular mean free path and the average speed of the molecules. By analogy, the turbulent viscosity can also be expressed as a product of the characteristic turbulent length and velocity scales (see also Hanjalic).[2]

Similar to the viscous stress for a Newtonian isotropic fluid the turbulent stress tensor is expressed by the use of a linear correlation between the strain rate tensor S_{ij} and the Reynolds stress tensor $-\rho\overline{u_i'u_j'}$ (Boussinesq hypothesis).

$$-\rho\overline{u_i'u_j'} = \rho c_\mu \, l \, v \, S_{ij} - \frac{2}{3}\rho k \delta_{ij} \qquad (3)$$

If the turbulent length scale is substituted by the turbulent time scale T the Reynolds stress tensor can be expressed by

$$-\rho\overline{u_i'u_j'} = c_{\mu,k\varepsilon}\, \rho v^2 T \, S_{ij} - \frac{2}{3}\rho k \delta_{ij} \qquad (4)$$

v describes the turbulent velocity scale, l the turbulent length scale, T the turbulent time scale and c_μ is a model constant. According to the molecular viscosity the turbulent viscosity μ_t can be expressed by:

$$\mu_t = \rho c_\mu \, l \, v = \rho c_\mu \, T \, v^2 \qquad (5)$$

The turbulent kinetic energy k is defined as follows:

$$k = 0.5\, \overline{u_k' u'}_k \qquad (6)$$

Standard $k-\varepsilon$ turbulence model

To close the linear eddy viscosity turbulence model the turbulent velocity scale and the turbulent length or time scale must be known. If the standard $k-\varepsilon$ turbulence model is used the time scale and the velocity scale are determined by the following equations:

$$T = \frac{k}{\varepsilon} \qquad (7)$$

$$v = \sqrt{k} \qquad (8)$$

Therefore the turbulent viscosity can be expressed by the well known relation

$$\mu_t = \rho c_\mu \frac{k^2}{\varepsilon}. \qquad (9)$$

[2] Instead of the product of characteristic turbulent length and velocity scales it is also possible to use the product of characteristic turbulent time and the square velocity scale.

The v2f turbulence model

The Boussinesq assumption in the standard $k-\varepsilon$ turbulence model is applied together with wall functions. But it is well known that in the near wall region the Standard $k-\varepsilon$ turbulence model must be modified via damping or wall functions. These functions are usually derived for simple flows, such as channel flows, and are ill-suited for most complex flows.

Based on this observation Durbin (1991) introduced an alternative eddy viscosity formulation, v2f-turbulence model, which uses an imaginary turbulent normal stress component $\overline{v'^2}$. This imaginary stress component is always normal to the closest wall and represents the turbulent velocity scale.

$$-\rho\overline{u_i'u_j'} = c_{\mu,v2f}\,\rho\overline{v'^2}T\,S_{ij} - \frac{2}{3}\rho k\delta_{ij} \quad (10)$$

In the v2f model the turbulent viscosity can be determined as follows:

$$\mu_t = \rho c_{\mu,v2f}\,\overline{v'^2}T \quad (11)$$

The transport equation for the normal-to-wall fluctuation velocity can be derived from the Reynolds stress equation with linear pressure strain model and the boundary layer simplifications. Because the pressure in a fluid flow is of elliptic nature and therefore the correlation of fluctuating pressure and fluctuating velocity gradient (the pressure-strain) is also elliptic the wall-reflection (redistribution of normal stresses near the wall) is considered by means of elliptic relaxation.

The original v2f model suggested by Durbin (1991, 1993, 1995) was numerically unstable using segregated solvers based on the pressure correction method. In order to make the v2f model suitable for segregated solvers (for incompressible flows) Lien and Kalitzin (2001) modified the model so that it becomes much more numerically attractive. The modified v2f turbulence model can be summarized in the following form:

$$\frac{\partial\overline{v'^2}}{\partial t} + u_j\frac{\partial\overline{v'^2}}{\partial x_j} = k\,f - 6\frac{\overline{v'^2}}{k}\varepsilon + \frac{\partial}{\partial x_j}\left(\left(\nu + \frac{\nu_t}{\sigma_k}\right)\frac{\partial\overline{v'^2}}{\partial x_j}\right) \quad (12)$$

$$L^2\frac{\partial^2 f}{\partial x_j^2} - f = \frac{C_1}{T}\left(\frac{\overline{v'^2}}{k} - \frac{2}{3}\right) - C_2\frac{P_k}{k} - \frac{1}{T}\left(6\frac{\overline{v'^2}}{k} - \frac{2}{3}\right) \quad (13)$$

$$P_k = 2\,C_\mu\,\overline{v'^2}\,T\,S_{ij}\,S_{ij}$$

The v2f model is based on the standard $k-\varepsilon$ equations with the eddy viscosity formulation according to equation (10). The turbulent time scale T and length scale L are given by

$$T = \max\left(\frac{k}{\varepsilon}, 6\sqrt{\frac{\nu}{\varepsilon}}\right) \quad (14)$$

$$L = C_L\max\left(\frac{k^{3/2}}{\varepsilon}, C_\eta\frac{\nu^{3/4}}{\varepsilon^{1/4}}\right) \quad (15)$$

The limits, expressed by Kolmogorov variables, are introduced in order to avoid singularities in the governing equations at solid walls and they are active only very close to walls (in this work $y^+ < 30$).

The wall boundary conditions for this model are:

$$u_j = k = \overline{v'^2} = f = 0$$

$$\varepsilon = 2\nu\left(\frac{k}{y_p^2}\right). \quad (16)$$

y_p is the distance from the cell centre to the wall.

At the inlet and outlet faces the fluxes of f were set to zero. For this work the following model constants for the v2f turbulence model were used:

$c_{\mu,v2f}$	$c_{\varepsilon,1}$	$c_{\varepsilon,2}$	c_1	c_2
0.22	1.4	1.9	1.4	0.3

σ_k	σ_ε	c_L	c_η
1.0	1.3	0.23	70

Table 2: Model constants for the used linear and nonlinear v2f turbulence model

It turns out that in the region far away from the wall, the Laplace term in the equation (13) is not negligible, and as a consequence $\overline{v'^2}$ gets too large so that $\overline{v'^2} > \frac{2}{3}k$.[3] For this reasons Davidson et al. (2003) proposed a simple modification to set an upper bound for the source term kf in the $\overline{v'^2}$ - equation as

$$\Phi_{\text{v2f,source}} = \min(kf, \Pi_{kf})$$

$$\Pi_{kf} = -\frac{1}{T}\left[(C_1 - 6)\overline{v'^2} - \frac{2}{3}k(C_1 - 1)\right] + C_2 P_k \quad (17)$$

This modification ensures that $\overline{v'^2} < 2/3k$. In regions where $\overline{v'^2} \approx 2/3k$ the v2f model predict the turbulent viscosity considerably larger as the standard $k-\varepsilon$ turbulence model so that Davidson et al. (2003) suggested a simple remedy to compute the turbulent viscosity:

$$\mu_t = \min\left\{\rho c_{\mu,ke}\frac{k^2}{\varepsilon}, \rho c_{\mu,v2f}\overline{v'^2}T\right\} \quad (18)$$

Nonlinear eddy viscosity concept

In addition to the differential Reynolds stress transport equations the turbulent stresses can be calculated by the use of

[3] $\overline{v'^2}$ is the imaginary turbulent normal stress component. Consequently it is the smallest normal stress component which is $\overline{v'^2} \le \frac{2}{3}k$.

nonlinear eddy viscosity concept. The most nonlinear models are defined by the use of the Reynolds stress anisotropy tensor b_{ij}.

$$b_{ij} = \frac{\overline{u_i' u_j'}}{2k} - \frac{1}{3}\delta_{ij} \quad (19)$$

The tensor b_{ij} is approximated with polynomial linear independent tensors T^{λ} of second order which can be built by strain-rate and rate-of-rotation tensor.

$$b_{ij} = \sum_{\lambda} G_{\lambda} T^{\lambda} \quad (20)$$

For 2-dimensional flows Pope (1975) and Speziale and Gatski (1992) showed that the Reynolds stress anisotropy tensor can be computed only with a second-order approximation of a complete non-linear relationship between the Reynolds-stress anisotropy tensor and the velocity gradients.

$$\begin{aligned} b_{ij} &= G_1 T\, S_{ij} \\ &+ G_2 T\left(S_{kj}\Omega_{ik} + \Omega_{jk} S_{ki}\right) \\ &+ G_3 T\left(S_{ik}S_{kj} - \frac{1}{3} S_{mn} S_{mn}\delta_{ij}\right) \end{aligned} \quad (21)$$

Where T represents the turbulent time scale and $G_{\lambda} = G_{\lambda}(\eta_1, \eta_2)$ are coefficients which are dependent on the dimensionless velocity gradient parameters

$$\eta_1 = T^2\left(S_{lk} S_{lk}\right) \quad (22)$$

$$\eta_2 = T^2\left(\Omega_{lk}\Omega_{lk}\right) \quad (23)$$

with

$$S_{ij} = \left(\frac{\partial u_i}{\partial x_j} + \frac{\partial u_j}{\partial x_i}\right) \quad (24)$$

$$\Omega_{ij} = \left(\frac{\partial u_i}{\partial x_j} - \frac{\partial u_j}{\partial x_i}\right) \quad (25)$$

All algebraic Reynolds-stress turbulence models (equation (20)) imply that the convective and diffusive transport of the Reynolds-stress anisotropy tensor b_{ij} is near to zero. This assumption is fulfilled in homogeneous turbulent flows and in flows with local equilibrium (production = dissipation).

Nonlinear eddy viscosity turbulence model by Ehrhard (1999)

Based on equation (21) for the Reynolds-stress anisotropy tensor Ehrhard (1999) developed a nonlinear $k-\varepsilon$ turbulence model which was calibrated by the use of simple two dimensional shear and complex flows with recirculation zones. The final form of the nonlinear $k-\varepsilon$ turbulence model is given by

$$
\begin{aligned}
\overline{u_i'u_j'} = {} & \frac{2}{3}k\delta_{ij} - 2C_\mu v^2\, T\, S_{ij} \\
& + C_1\, C_\mu v^2\, T^2\left(S_{ik}S_{kj} - \frac{1}{3}S_{kl}S_{kl}\delta_{ij}\right) + C_2\, C_{\mu,ke} v^2\, T^2\left(\Omega_{ik}S_{kj} - \Omega_{jk}S_{ki}\right) \\
& + C_3\, C_\mu v^2\, T^2\left(\Omega_{ik}\Omega_{jk} - \frac{1}{3}\Omega_{lk}\Omega_{lk}\delta_{ij}\right) + C_4\, C_{\mu,ke} v^2\, T^3\left(S_{ki}\Omega_{lj} - S_{kj}\Omega_{li}\right)S_{kl} \\
& + C_5\, C_\mu v^2\, T^3\left(\Omega_{il}\Omega_{lm}S_{mj} + S_{il}\Omega_{lm}\Omega_{mj} - \frac{2}{3}S_{lm}\Omega_{mn}\Omega_{nl}\delta_{ij}\right) \\
& + C_6\, C_\mu v^2\, T^3 S_{ij}S_{kl}S_{kl} \\
& + C_7\, C_\mu v^2\, T^3 S_{ij}\Omega_{kl}\Omega_{kl}
\end{aligned}
\qquad (26)
$$

$$
C_\mu = \min\left(\frac{1}{0.9S^{1.4} + 0.4\Omega^{1.4} + 3.5}\ , 0.15\right),\ S = \frac{k}{\varepsilon}\sqrt{2S_{ij}S_{ij}}\ ,\ \Omega = \frac{k}{\varepsilon}\sqrt{2\Omega_{ij}\Omega_{ij}}
$$

$$
C_1 = -0.2\,,\ C_2 = 0.4\,,\ C_3 = 2.0 - \exp\left(-\left(S-\Omega\right)^2\right),\ C_4 = -32.0\ C_\mu^2,\ C_5 = 0.0
$$

$$
C_6 = -16.0\ C_\mu^2,\ C_7 = 16.0\ C_\mu^2
$$

The boundary conditions and the model constants are the same as by the standard $k-\varepsilon$ turbulence model. The model constants for the k and ε equations are equal the default settings in Fluent. But the production term is determined as follows:

$$
P_k = -\rho\overline{u_i'u_j'}\frac{\partial u_j}{\partial x_i} \qquad (27)
$$

Nonlinear eddy viscosity turbulence model by Lübcke et al. (2003)

Lübcke et al. (2003) also developed the projection method of a nonlinear $k-\varepsilon$ turbulence model with the focus to improve the prediction of the lateral spreading rate from three dimensional wall jets. The original model based on the low-Re $k-\varepsilon$ turbulence model was reported by Lien and Leschziner (1993). In this paper wall functions are used to reduce the computational effort. The boundary conditions and the modelling of the production term are the same as in the nonlinear model from Ehrhard (1999). The final form of the nonlinear $k-\varepsilon$ turbulence model by Lübcke et al. (2003) is given by equation (28)

$$
\begin{aligned}
b_{ij} &= -2C_\mu T\left(S_{ij} + \beta_2 T\left[S_{ik}W_{kj} - W_{ik}S_{kj}\right]\right) \\
&\quad - \beta_3 T\left(S_{ik}S_{kj} - \frac{1}{3}S_{kq}S_{qk}\delta_{ij}\right) + \beta_5 T^2\left(\Omega_{ik}S_{kl}S_{lj} - S_{ik}S_{kl}W_{lj}\right) \\
&\quad + \beta_8 T^3\left(S_{ik}\Omega_{kl}S_{lq}S_{qj} - S_{ik}S_{kl}W_{lq}S_{qj} - \frac{1}{2}S_{pm}S_{mp}\left[S_{ik}\Omega_{kj} - \Omega_{ik}S_{kj}\right]\right) \\
C_\mu &= \frac{-A_1 g}{g^2 - \frac{2}{3}A_3^2\eta_1 - 2A_2^2\eta_2} \\
\beta_2 &= -A_2/g, \quad \beta_3 = -2A_3/g, \quad \beta_5 = \frac{-6A_2\left(A_3 - A_2\sqrt{-\eta_2/\eta_1}\right)}{-2g^2 + A_3^2\eta_1 + A_2^2\eta_2}, \quad \beta_8 = C^8\frac{-6A_2}{\eta_1 g} \\
\eta_1 &= T^2 S_{ik}S_{ki}, \; \eta_2 = T^2\Omega_{ik}\Omega_{ki}, \; g = C_1 - 2T\left(b_{ik}S_{ki}\right) - 1 \\
A_1 &= \frac{1}{2}C_2 - \frac{2}{3}, \; A_2 = \frac{1}{2}C_4 - 1, \; A_3 = \frac{1}{2}C_3 - 1 \\
C_1 &= 2.5, \; C_2 = 0.39, \; C_3 = 1.25, \; C_4 = 0.45, \; C_8 = -1
\end{aligned}
\tag{28}
$$

Nonlinear v2f eddy viscosity turbulence model by Pettersson Reif (1999)

Based on the nonlinear relationship between the Reynolds-stress anisotropy tensor and the velocity gradients (see equation (21)) Pettersson Reif (1999) developed an internally consistent nonlinear v2f model. This model ensures the realizability constraints ($\overline{u'^2_\alpha} \geq 0$, $\overline{u'^2_\alpha} \leq 2k$ and $\left(\overline{u'_\alpha u'_\beta}\right)^2 \leq \overline{u'^2_\alpha}\,\overline{u'^2_\beta}$) so that in parallel shear flows the normal-to-wall Reynoldsstress component is equal to the imaginary stress component $\overline{v'^2}$. Based on equation (21) for the Reynolds-stress anisotropy tensor the final form of the nonlinear v2f turbulence model is given by

$$\overline{u_i'u_j'} = \frac{2}{3}k\delta_{ij} - 2C_{\mu,1}\overline{v'^2}\,T\,S_{ij}$$
$$-V\,k\,T^2\left[C_{\mu,2}\left(S_{ik}\Omega_{kj} + S_{jk}\Omega_{ki}\right) - C_{\mu,3}\left(S_{ik}S_{kj} - \frac{1}{3}S_{mn}S_{mn}\delta_{ij}\right)\right]$$

$$C_{\mu,1} = C_{\mu,v2f}\,,\ \ C_{\mu,2} = \frac{6}{5}\frac{\sqrt{1-\left(C_{\mu,1}\frac{\overline{v'^2}}{k}\right)^2 2\eta_1}}{\beta_1 + \sqrt{\eta_1\eta_2}}\,,\ \ C_{\mu,3} = \frac{6/5}{\gamma_1 + \eta_1} \qquad (29)$$

$$V = \max\left[\frac{2}{3} - \frac{\overline{v'^2}}{k}, 0\right],\ \ \beta_1 = \frac{1}{0.1 + \sqrt{\eta_1\eta_2}}\,,\ \ \gamma_1 = \frac{1}{0.1 + \eta_1}$$

The boundary conditions and the model constants are the same as in the linear turbulence model. The production term is determined by equation (27).

Differential Reynolds stress turbulence models

The differential Reynolds stress model (RSM) represents a more general turbulence model. It uses for every turbulent stress an own transport equation. For incompressible and isothermal flows without system rotation the RSM model takes the following form:

$$\frac{D\left(\overline{u_i'u_j'}\right)}{Dt} = D_{ij}^T + D_{ij}^L + P_{ij} + \phi_{ij} - \varepsilon_{ij} \qquad (30)$$

Where D_{ij}^T, D_{ij}^L, P_{ij}, ϕ_{ij} are turbulent diffusion, molecular diffusion, stress production and pressure strain terms and ε_{ij} is the dissipation tensor. To close the equations the terms D_{ij}^T, ϕ_{ij} and ε_{ij} need to be modelled. In this work the commercial CFD code FLUENT was used. That implies that the turbulent diffusion and the dissipation tensor are simplified as follows:

$$D_{ij}^T = \frac{\partial}{\partial x_k}\left(\frac{\nu_t}{\sigma_k}\frac{\partial\overline{u_i'u_j'}}{\partial x_k}\right) \qquad (31)$$
$$\varepsilon_{ij} = \frac{2}{3}\delta_{ij}\varepsilon$$

In general the pressure strain term can be computed by the following decomposition:

$$\phi_{ij} = \phi_{ij,1} + \phi_{ij,2} + \phi_{ij,w} \qquad (32)$$

The first term $\phi_{ij,1}$ refers to the “turbulence interaction” part of the pressure strain process and is called “the slow pressure strain term”. The slow term describes the interaction between the pressure and velocity fluctuations. The second term $\phi_{ij,2}$ is called the mean strain or “rapid” contribution for the pressure strain process and describes the interaction between the pressure and the time-averaged velocity field. If the flow regions are influenced by rigid walls the third term ϕ_w must be included. This term considers the reflection of pressure fluctuations near walls which are responsible for the redistribution of normal stresses.

In FLUENT two pressure-strain models are available. The most commonly used model is the linear pressure strain model (IP) according to the proposal by Gibson and Launder (1978), Fu et al. (1987) and Launder (1989). In near wall regions a low Reynolds modification by Launder and Shima (1989) is also available. Additional to the linear model a quadratic pressure strain model (SSG) proposed by Speziale et al. (1991) is provided in FLUENT. A detailed description of the models can be found in the FLUENT manual (FLUENT, 2001).

In this work two another higher order pressure-strain models and one enhanced wall reflection term were used. The models use the anisotropy invariants and Lumley’s flatness parameter to consider the different limiting behaviour for the Reynolds stress components.

$$a_{ij} = \frac{\overline{u_i' u_j'}}{k} - \frac{2}{3}\delta_{ij}$$

$$A_2 = a_{ij} a_{ij}, \; A_3 = a_{ij} a_{jk} a_{ki} \tag{33}$$

$$A = 1 - \frac{9}{8}\left(A_2 - A_3\right)$$

The models are implemented in FLUENT via compiled user defined function (UDF).

Cubic pressure strain model by Craft et al. (1993)

The first model was proposed by Craft et al. (1993) for impinging jet studies and is called “cubic model”. This model is based on a commonly used wall reflection term ϕ_w (Craft and Launder, 1992) to satisfy the redistribution of normal stresses near the wall. The cubic pressure strain model can be summarized as follows:

$$\phi_{ij,1} = -c_1\varepsilon\left(a_{ij} + c_1'\left(a_{ik}a_{jk} - \frac{1}{3}A_2\delta_{ij}\right)\right) - \varepsilon\, a_{ij}$$

$$\begin{aligned}\phi_{ij,2} = &-0.6\left(P_{ij} - \frac{1}{3}\delta_{ij}P_{kk}\right) + 0.3\,a_{ij}P_{kk} \\ &-0.2\left[\frac{\overline{u_k'u_j'}\,\overline{u_l'u_i'}}{k}\left(\frac{\partial u_k}{\partial x_l} + \frac{\partial u_l}{\partial x_k}\right) - \frac{\overline{u_l'u_k'}}{k}\left(\overline{u_i'u_k'}\frac{\partial u_j}{\partial x_l} + \overline{u_j'u_k'}\frac{\partial u_i}{\partial x_l}\right)\right] \\ &-0.6\left[A_2\left(P_{ij} - D_{ij}\right) + 3\,a_{mi}a_{nj}\left(P_{mn} - D_{mn}\right)\right]\end{aligned}$$

$$\begin{aligned}\phi_{ij,w} = \; & c_{w,1}'\frac{\varepsilon}{k}\left(\overline{u_k'u_m'}\,n_k n_m\delta_{ij} - \frac{3}{2}\overline{u_k'u_i'}\,n_k n_j - \frac{3}{2}\overline{u_k'u_j'}\,n_i n_k\right)\frac{k^{3/2}}{2.55\,x_n\,\varepsilon} \\ &+ c_{w,2}'\left(\phi_{km,2}\,n_k n_m\delta_{ij} - \frac{3}{2}\phi_{ik,2}\,n_k n_j - \frac{3}{2}\phi_{kj,2}\,n_i n_k\right)\frac{k^{3/2}}{2.55\,x_n\,\varepsilon}\end{aligned} \qquad (34)$$

$$c_1 = 3.1\left(A_2 A\right)^{1/2},\; c_1' = 1.2$$

$$D_{ij} = -\left(\overline{u_i'u_k'}\frac{\partial u_k}{\partial x_j} + \overline{u_j'u_k'}\frac{\partial u_k}{\partial x_i}\right)$$

TCL pressure strain model by Craft and Launder (2001)

The second pressure strain model is more widely applicable and satisfies the two-component limit (TCL). The turbulence reduces at a wall without a wall-correction term $\phi_{ij,w}$.This approach was devised to free shear flows, but has recently been applied to quite complicate flows in ducts and pipe bends with better agreements as the IP pressure strain model (Craft and Launder 2001). The TCL pressure strain model takes the following form:

$$
\begin{aligned}
\phi_{ij,1} &= -c_1 \varepsilon \left(a_{ij} + c_1' \left(a_{ik} a_{jk} - \frac{1}{3} A_2 \delta_{ij} \right) \right) - \varepsilon a_{ij} \\
\phi_{ij,2} &= -0.6 \left(P_{ij} - \frac{1}{3} \delta_{ij} P_{kk} \right) + 0.3 a_{ij} P_{kk} \\
&\quad - 0.2 \left[\frac{\overline{u_k' u_j'}\,\overline{u_l' u_i'}}{k} \left(\frac{\partial u_k}{\partial x_l} + \frac{\partial u_l}{\partial x_k} \right) - \frac{\overline{u_l' u_k'}}{k} \left(\overline{u_i' u_k'} \frac{\partial u_j}{\partial x_l} + \overline{u_j' u_k'} \frac{\partial u_i}{\partial x_l} \right) \right] \\
&\quad - c_2 \left[A_2 \left(P_{ij} - D_{ij} \right) + 3 a_{mi} a_{nj} \left(P_{mn} - D_{mn} \right) \right] \\
&\quad + c_2' \left(\Pi_1 + \Pi_2 + \Pi_3 + \Pi_4 + \Pi_5 \right) \\
\Pi_1 &= \left(\frac{7}{15} - \frac{A_2}{4} \right) \left(P_{ij} - \frac{1}{3} \delta_{ij} P_{kk} \right) \\
\Pi_2 &= 0.1 \left[a_{ij} - \frac{1}{2} \left(a_{ik} a_{kj} - \frac{1}{3} \delta_{ij} A_2 \right) \right] P_{kk} - 0.05 a_{ij} a_{lk} P_{kl} \\
\Pi_3 &= 0.1 \left[\left(\frac{\overline{u_i' u_m'}}{k} P_{mj} + \frac{\overline{u_j' u_m'}}{k} P_{mi} \right) - \frac{2}{3} \delta_{ij} \frac{\overline{u_l' u_m'}}{k} P_{ml} \right] \qquad (35) \\
\Pi_4 &= 0.2 \frac{\overline{u_l' u_i'}\,\overline{u_k' u_j'}}{k^2} \left(D_{lk} - P_{lk} \right) \\
\Pi_5 &= 0.1 \left[\frac{\overline{u_l' u_i'}\,\overline{u_k' u_j'}}{k^2} - \frac{1}{3} \delta_{ij} \frac{\overline{u_l' u_m'}\,\overline{u_k' u_m'}}{k^2} \right] \times \left[6 D_{lk} + 13 k \left[\frac{\partial u_l}{\partial x_k} + \frac{\partial u_k}{\partial x_l} \right] \right] \\
c_1 &= 3.1 \left(A_2 A \right)^{1/2}, \; c_1' = 1.1 \\
c_2 &= \min \left(0.55 \left(1 - \exp \left(- A^{1.5} R_t / 100 \right) \right), 3.2 A / \left(1 + S \right) \right) \\
c_2' &= \min \left(0.6, A \right) + 3.5 \left(S - \Omega \right) / \left(3 + S + \Omega \right) - 2 S_I \\
S &= \frac{k}{\varepsilon} \sqrt{S_{ij} S_{ij} / 2}, \; \Omega = \frac{k}{\varepsilon} \sqrt{\Omega_{ij} \Omega_{ij} / 2}, \; S_I = S_{ij} S_{jk} S_{ki} / \left(S_{st} S_{st} / 2 \right)^{1.5}
\end{aligned}
$$

Wall reflection term by Craft and Launder (1992)

The IP and cubic pressure strain models need a wall reflection term ϕ_w to consider the redistribution of normal stresses near the wall. Beside the standard wall reflection term (equation (34)) a proposal from Craft and Launder (1992) is adopted. This wall reflection term was devised to cope both with parallel shear flows and with impinging flows (Craft and Launder, 2001) and has the following form:

$$\begin{aligned}\phi_{ij,w} = & -0.08 \frac{\partial u_l}{\partial x_m} \overline{u_l' u_m'} \left(n_q n_q \delta_{ij} - 3 n_i n_j \right) \frac{k^{3/2}}{2.55 x_n \, \varepsilon} \\ & -0.10 k \left(\frac{\partial u_k}{\partial x_m} n_l n_k a_{lm} \delta_{ij} - \frac{2}{3} \frac{\partial u_i}{\partial x_m} n_l n_j a_{lm} - \frac{2}{3} \frac{\partial u_j}{\partial x_m} n_l n_i a_{lm} \right) \frac{k^{3/2}}{2.55 x_n \, \varepsilon} \\ & +0.40 k \frac{\partial u_l}{\partial x_m} n_l n_m \left(n_i n_j - \frac{1}{3} n_q n_q \delta_{ij} \right) \frac{k^{3/2}}{2.55 x_n \, \varepsilon}\end{aligned} \qquad (36)$$

This wall reflection term was also implemented in FLUENT via compiled user defined function.

Hybrid Reynolds Stress turbulence models

Prandtl's second kind of secondary motion (Craft and Launder, 2001) in squared duct flows and three dimensional wall jets is mainly forced by the anisotropic turbulent normal stresses $-\rho \overline{u_i' u_j'}$. For this reason and to reduce the computational effort, a hybrid RSM turbulence model is proposed which determines the turbulent shear stresses by using the Boussinesq assumption and the turbulent normal stresses by transport equations.

for $i \neq j$

$$\overline{u_i' u_j'} = -2 C_{\mu,ke} \, k \, T \, S_{ij} \qquad (37)$$

for $i = j$

$$\frac{D\left(\overline{u_i' u_j'}\right)}{Dt} = D_{ij}^T + D_{ij}^L + P_{ij} + \phi_{ij} - \varepsilon_{ij}$$

Another advantage of the hybrid turbulence model is that it is more stable as the full Reynolds stress turbulence model.

Implementation of the described turbulence models

In Fluent a wide range of turbulence models are implemented. To analyse the potential of improvement for the prediction of Prandtl's second kind of secondary motion additional turbulence models were implemented in Fluent via compiled user defined functions.

The transport equations for the v2f turbulence models were implemented via user defined scalars. Because Fluent provides the direct definition of the advective and diffusivity terms the implementation in the Fluent code is very simple. The boundary conditions for the transport quantities can also be defined directly via user defined functions.

The different pressure strain models were implemented by the definition of source terms for the different transport stress-equations. The hybrid Reynolds stress turbulence model was implemented by a defined adjust routine which computes the turbulent shear stresses with the Boussinesq assumption. The computed shear stresses are connected with the calculation domain by the use of fixed value definitions.

Some turbulence models are easier to implement by the use of auxiliary variables. For example the v2f turbulence model uses information about the turbulent time and length scale. For this reason the user defined scalars and also the user defined memory are used.

Because the nonlinear turbulence models are sometimes numerical unstable, the calculation of the production term was modified so that at start of the iteration procedure a linear correlation between the Reynolds stresses and the deformation tensor was used. For this reason the production term was stored also in a user defined memory to easier switch between the Boussinesq assumption and equation (27).

The source code of all in this paper used UDFs can be downloaded from the Homepage of the Fachhochschulstudien-gänge Burgenland GmbH (www.fh-pinkafeld.ac.at/fhplus/ download.htm).

Comparison of the turbulence models

Two dimensional turbulent channel flow

The correct implementation of the different turbulence and pressure strain models was tested with the prediction of the normal and shear stresses in a channel flow with an turbulent Reynolds-number of $\mathrm{Re}_\tau = 590$ and compared with the DNS data of Moser (1999). Because some models use wall functions and some use a low Reynolds enhanced treatment two different grids were designed. The grid for the low-Re models was designed with a $y^+ < 1$ and the other grid with a $y^+ \approx 60$. Figure 1 to Figure 5 show the computed results for the turbulent kinetic energy and the Reynolds stresses for both grids.

The value $y/(0.5h) = 0$ on the abscissa denotes the channel centre.

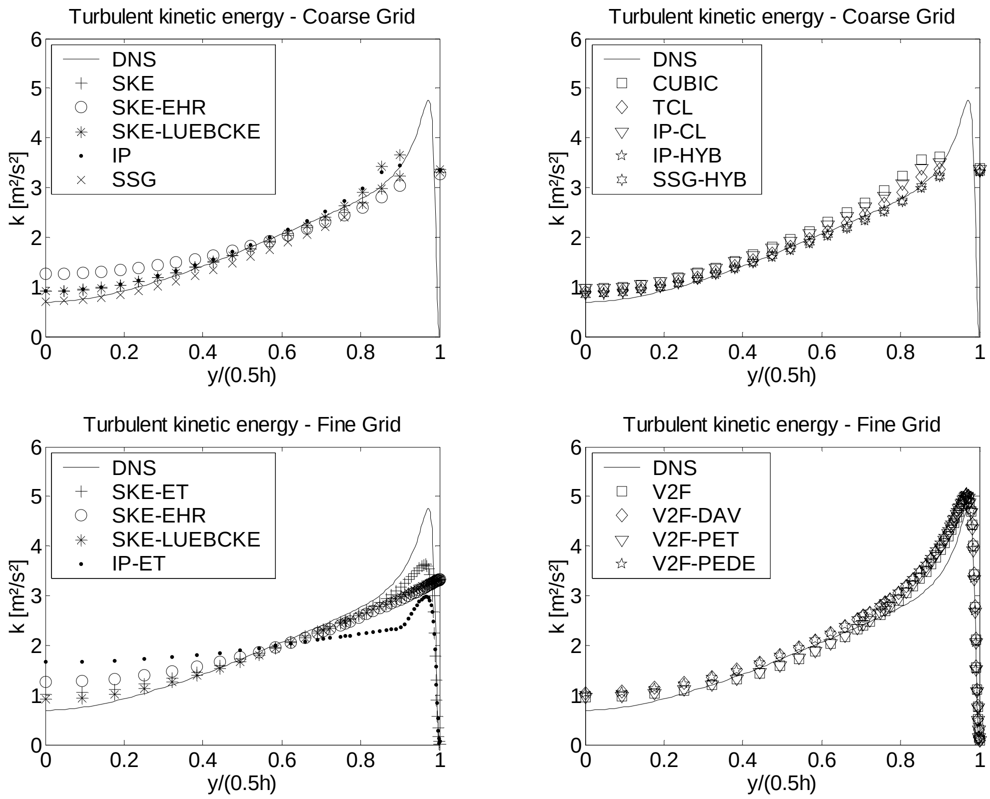

Figure 1: Turbulent kinetic Energy k [m²/s²]

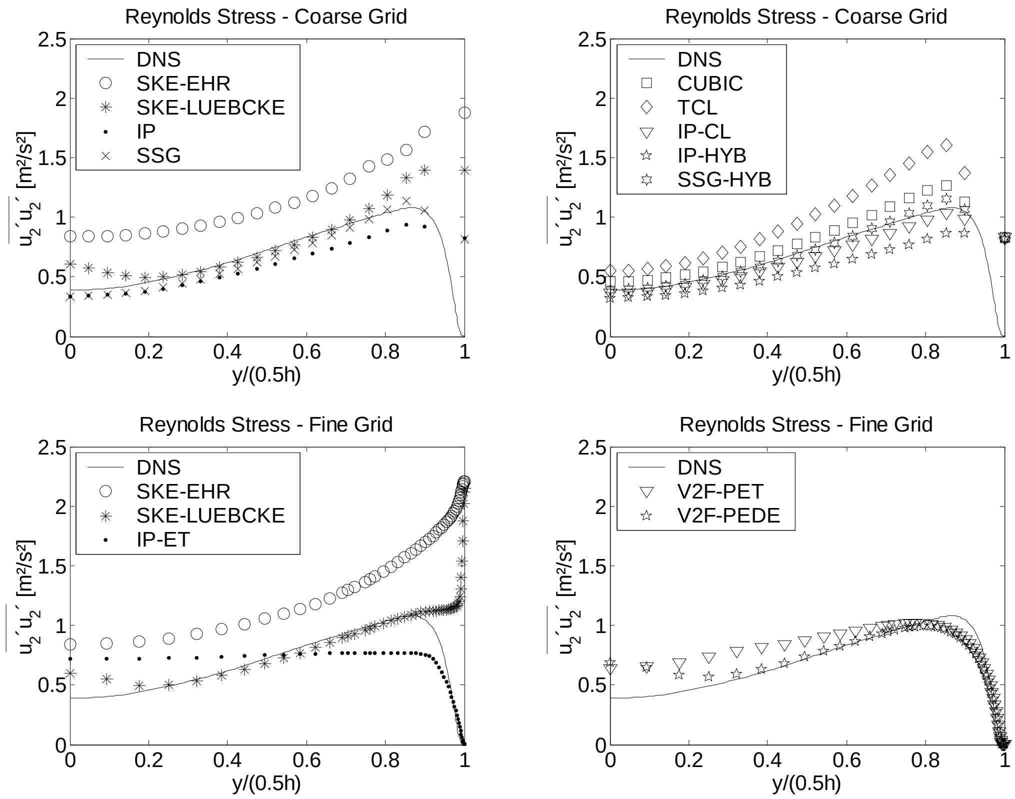

Figure 2: Reynolds Stress in wall normal direction ($\overline{u_2'u_2'}$ [m²/s²])

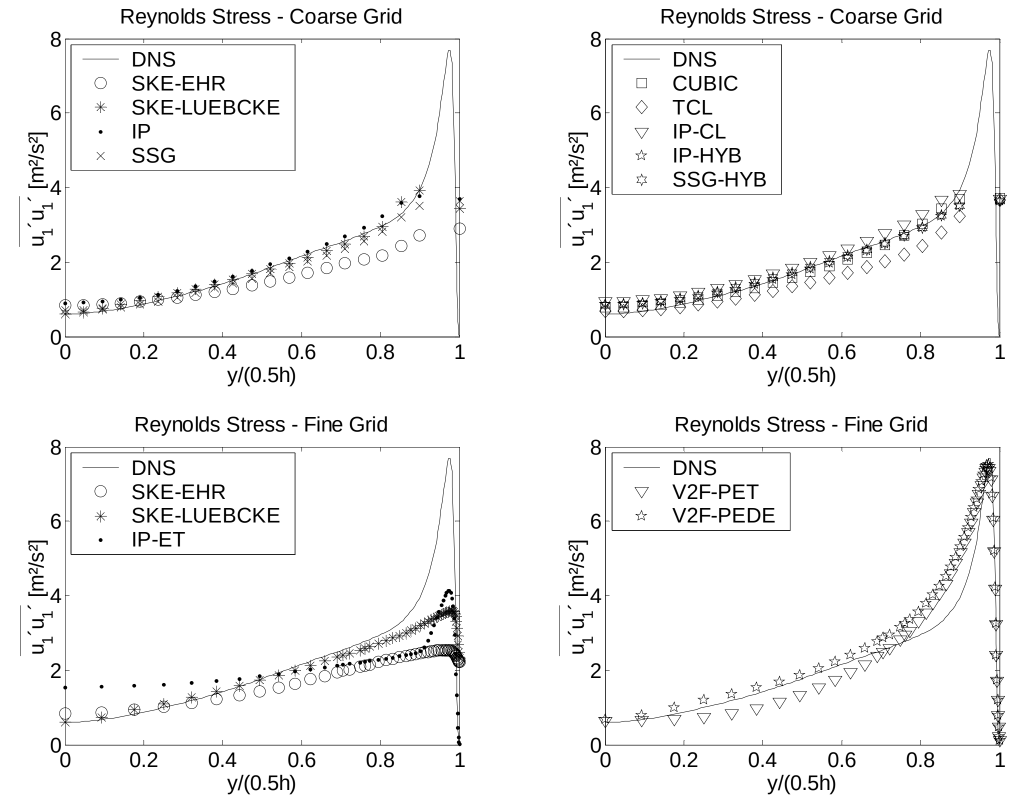

Figure 3: Reynolds Stress in mean flow direction ($\overline{u_1'u_1'}$ [m²/s²])

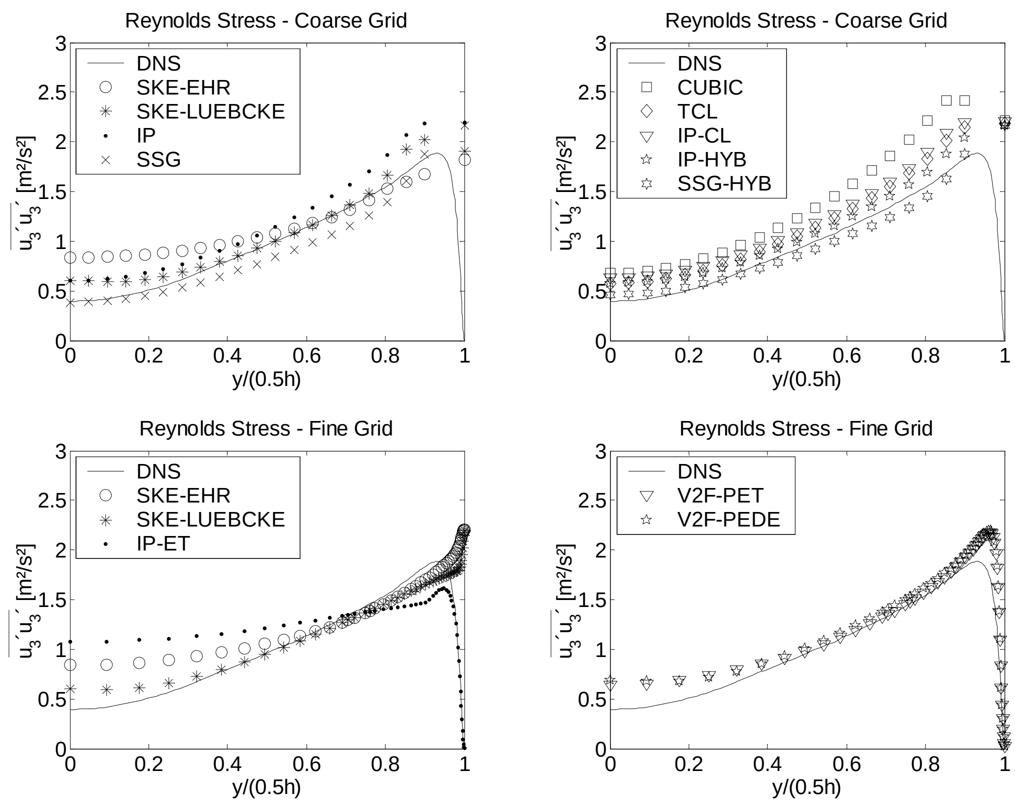

Figure 4: Reynolds Stress in lateral direction ($\overline{u_3'u_3'}$ [m²/s²])

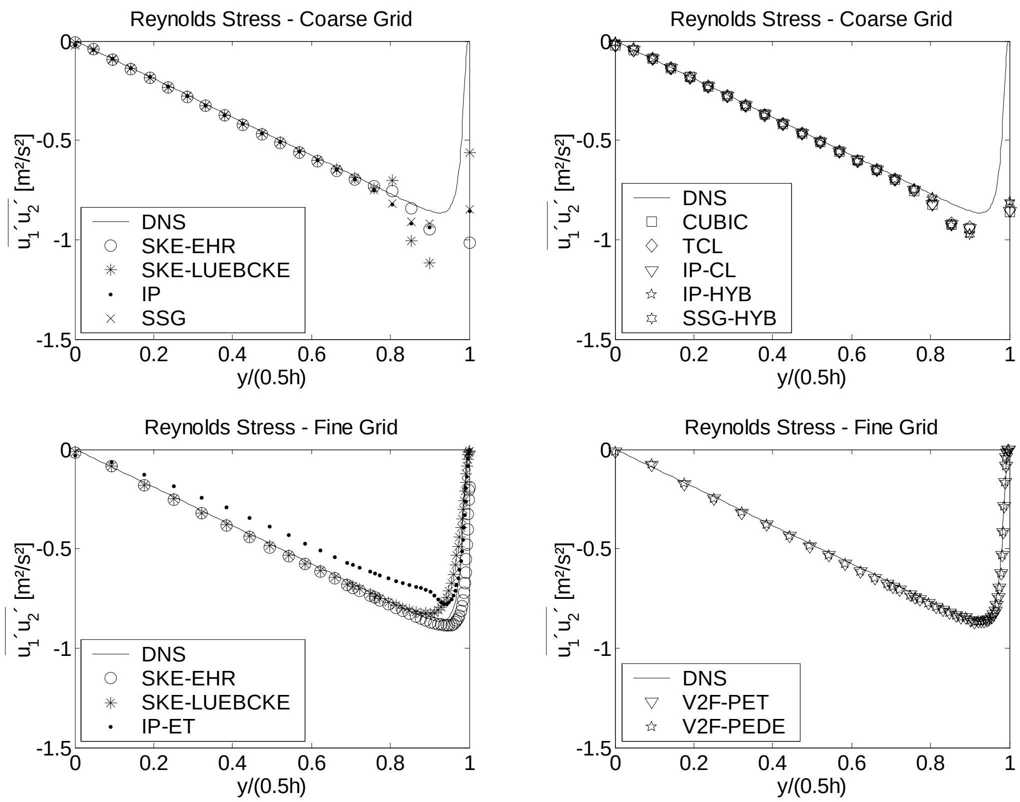

Figure 5: Reynolds Stress in lateral direction ($\overline{u_1'u_2'}$ [m²/s²])

For the coarser grid all turbulence models predict the turbulent kinetic energy near the wall well. In the middle of the channel the nonlinear eddy viscosity models predict a turbulence level which is too high. Especially the model by Ehrhard (SKE-EHR) – which was calibrated for simple and complex shear flows – has obvious differences to the DNS data. The Reynolds stresses are predicted well by the use of the full IP, SSG and the hybrid SSG turbulence model. The TCL and the cubic pressure strain model overpredict the lateral and the normal-to-the wall Reynolds stress components $\overline{u_2'u_2'}$ and $\overline{u_3'u_3'}$. The nonlinear turbulence models by Ehrhard (1999) and Lübcke (2003) show abnormalities. The reasons for the abnormalities can be founded in the different modelling of the k and ε equations. In this work the standard $k-\varepsilon$ model is used, but in the original model a low Reynolds extension was used. In the near wall region this has considerable effects especially for the fine grid.

With the fine grid the near wall behaviour is well predicted by the v2f models. The v2f model can predict the peak of the turbulent kinetic energy and in the nonlinear version the Reynolds Stress in mean flow direction $\overline{u_1'u_1'}$. But the computed results strongly depend on the time and length scale limit which are determined by equations (14) and (15). In this work the equations are activated only near the wall in the region $y^+ < 30$. Smaller values of y^+ are reducing the increase of the Reynolds stress $\overline{u_1' u_1'}$ and thereby the turbulent kinetic energy in the near wall region.

Three dimensional wall jet

As mentioned in the introduction Craft and Launder (2001) showed that the high lateral rate of spread can be attributed to stress-induced axial vorticity, which is generated by the anisotropy of the Reynolds normal stresses perpendicular to the jet axis.

For two dimensional channel flow the second moment closure models predict the turbulent anisotropy well. So it can be expected that the computed lateral spreading rate will also agree with the experimental data. However, most turbulence models are tuned by flat plate and channel flows so that further validations are necessary.

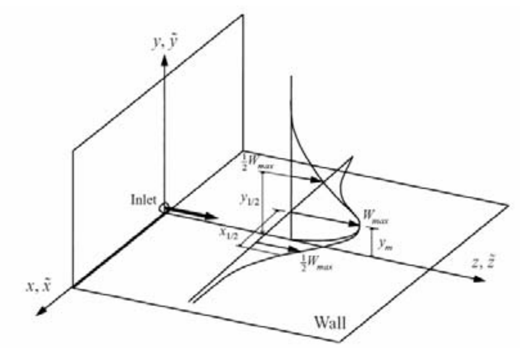

Figure 6: Investigated flow situation (Craft and Launder, 1992)

For these investigations the experimental data of Abrahamsson (1997) was used. The experimental setup is shown in Figure 6, where it is noticed that the three dimensional wall jet is allowed to develop over a large surface (width 3.2m and length 2.1m).

The flow is injected out of a circular orifice at the wall with a diameter of 20mm. The below edge of the orifice was direct on the wall. The inlet is designed with a contraction which ensures a uniform velocity profile with a low turbulence level. The experimental data was generated for an inlet velocity of 60m/s. The 1.2m high wall over the inlet orifice give a well-defined boundary condition.

For the computation of the three dimensional wall jet two grids were designed. One coarse grid with $y^+ = 30 - 120$ and one fine grid with $y^+ = 1 - 6$. The coarse grid was used for the high Reynolds number turbulence models with wall functions and the fine grid was used for the low Reynolds number turbulence model with near wall treatments. The inlet area was designed with a prism volumes and the main flow domain with orthogonal hexahedron volumes. The interface between the different cell geometries was built with a nonconformal grid.

model	$\frac{dy_{1/2}}{dz}$	$\frac{dx_{1/2}}{dz}$	$\frac{\dot{x}_{1/2}}{\dot{y}_{1/2}}$
Experiment (Abrahamsson et al. 1997)	0.065	0.320	4.94
cubic	0.039	0.743	19.04
ip	0.043	0.913	21.36
ip-hyb	0.044	0.550	12.43
ip-without wr	0.078	0.089	1.15
ip-with-wr-LS	0.032	0.723	22.37
ske	0.074	0.070	0.95
ssg	0.057	0.049	0.85
tcl	0.038	0.743	19.30
ske-ewt	0.071	0.068	0.96
v2f-nonlinear	0.071	0.420	1.07

Table 3: Comparison of spreading rate anlong the jet

The computational results are summarized in Table 3. In contrast to the results of other authors (e.g. Craft and Launder, 2001) the presented spreading rates differ. A reason can be the poor convergence behavior of the used coarse grid (the residuum of the continuity was about 0.1). Especially the nonlinear eddy viscosity models by Lübcke (ske-lue) and Ehrhard (ske-ehr) were numerically unstable.

The results show the well known behavior of the different used turbulence models. The linear eddy viscosity turbulence model (for example the standard $k-\varepsilon$ turbulence model) and the simple isotropic pressure strain model (IP) are not able to predict the correct lateral spreading rate. This indicates that the wall reflection effect is not predicted satisfactorily.

Summary

The correct prediction of three dimensional wall jets is important for many industrial flow applications. Especially for ventilation systems which are mounted just below the ceiling the anisotropy of the Reynolds stresses can induce secondary motion which has an important influence on the flow distribution in the occupied zone.

Beside the standard turbulence models additional nonlinear eddy viscosity models and higher order pressure strain models were implemented in Fluent via compiled user defined functions. The implementation was verified with DNS data from a two dimensional turbulent channel flow. All implemented pressure strain models showed good agreement with the DNS data. But just one of the three implemented nonlinear eddy viscosity turbulence model – the nonlinear v2f - showed also good agreement.

The implemented turbulence and pressure strain models were also tested for a three dimensional wall jet. In this test case a complex hybrid mesh was used to test the numerical stabilities and the correct prediction of the considerable lateral spreading rate. The implemented pressure strain models and the nonlinear v2f turbulence models were stable but had poor convergence behaviour for the used

coarse grid. In addition, the quality of the flow prediction could not be improved, so that it can be outlined, that the in Fluent available turbulence models are a good compromise between stability and accuracy.

Nomenclature

k	m²/s²	Turbulent kinetic energy
p	Pa	Pressure
P_k	W/m³	Production term
Re		Reynolds number
S	1/s	Deformationsinvariante
S_ϕ		Source term of general fluid property
S_{ij}	s-1	Magnitude of the rate of strain
T	s	Timescale
u_i	m/s	Index notation of velocity components
$\overline{u}_i$	m/s	Average velocity
$\overline{u'_i u'_j}$	m²/s²	Doppel correlation tensor
y^+		Dimensionless wall distance
ρ	kg/m³	Density
β	1/K	Volumetric thermal expansion coefficient
μ	Pa s	Dynamic viscosity
ν	m²/s	Kinematic viscosity
$\phi_{ij,1}$		Slow pressure strain term for RSM model

$\phi_{ij,2}$		Rapid pressure strain term for RSM model
$\phi_{ij,w}$		Wall reflection term for RSM model
δ_{ij}		Kronecker delta function
σ_t		Model constant - turbulent Prandtl number
μ_t	Pa s	Turbulent dynamic viscosity
ε	m^2/s^3	Dissipation rate
Ω_{ij}		Rotation tensor
Ω		Vorticity invariant
κ		Von Karman's constant (0.42)

References

Abrahamsson H. (1997): On Turbulent Wall Jets. PhD thesis, Department of Thermo and Fluid Dynamics, Chalmers University of Technology, Göteburg Sweden. ISBN 91-7197-491-1

Craft T.J., Launder B.E. (1992): New wall-reflection model applied to the turbulent impinging jet. AIAA Journal, Vol. 30, Pages 2970-2972.

Craft T.J., Launder B.E. (2001): On the spreading mechanism of the three-dimensional turbulent wall jet. Journal of Fluid Mechanics, Vol. 435, Pages 305-326.

Davidson L., Nielsen P.V. and Sveningsson A. (2003): Modification of the v2f model for computing the flow in a 3D wall jet. Turbulence, Heat and Mass Transfer, Vol. 4, Pages 577-584

Durbin, P. (1991): Near-wall turbulence closure modeling without damping functions. Theoretical and Computational Fluid Dynamics 3, 1–13.

Durbin, P. (1993): Application of a near-wall turbulence model to boundary layers and heat transfer. International Journal of Heat and Fluid Flow 14, 316–323.

Durbin, P. (1995): Separated flow computations with the v2f model. AIAA Journal 33, 659–664.

Ehrhard J. (1999): Untersuchung linearer und nichtlinearer Wirbelviskositätsmodelle zur Berechnung turbulenter Strömungen um Gebäude. VDI Verlag Düsseldorf, Fortschrittsbericht VDI Reihe 7 Nr. 367ISBN 3-18-336707-6

FLUENT (2001): FLUENT 6.0 User's Guide, *Fluent Inc. Centerra Resource Park,* Lebanon

Fu S., Launder B.E. and Leschziner M.A. (1987): Modeling Strongly Swirling Recirculating Jet Flow with Reynolds-Stress Transport Closures. In Sixth Symposium on Turbulent Shear Flows, Toulouse, France

Gibson M.M. and Launder B.E. (1978): Ground Effects on Pressure Fluctuations in the Atmospheric Boundary Layer. J. Fluid Mech., 86:491-511.

Kalitzin, G. (1999): Application of the v2f model to aerospace configurations. Center for Turbulence Research Annual Research Briefs.

Launder B.E. (1989): Second-Moment Closure and Its Use in Modeling Turbulent Industrial Flows. International Journal for Numerical Methods in Fluids, 9:963-985

Launder B.E. and Shima N. (1989): Second-Moment Closure for the Near-Wall Sublayer: Development and Application. AIAA Journal, 27(10):1319-1325

Launder B.E., Rodi W. (1983): The turbulent wall jet. Annual Review Fluid Mechanics, Vol. 15, Page 429

Lien F.S. and Leschziner M.A. (1993): Computational modelling of 3d turbulent flow in s-diffuser and transition ducts. Engineering Turbulence Modelling and Experiments, Page 217

Lübcke, H.M., Rung Th., Thiele F. (2003): Prediction of the spreading mechanism of 3D turbulent wall jets with explicit Reynolds-stress closure, International Journal of Heat and Fluid Flow, Vol. 24, Pages 434-443

Moser R.D., Kim J., Mansour N. (1999): DNS of turbulent channel flow up to $\mathrm{Re}_\tau = 590$. Physics of Fluids. Vol. 111, N4, Pages 943-945

Newman B.G., Patel R.P., Savage S.B., Tjio H.K. (1972): Three dimensional wall jet originating from a circular orifice. Aeronaut. Q. 23, Page 187

Pettersson Reif B.A. (1999): A nonlinear constitutive relationship for the v2f model. Center for Turbulence Research, Annual Research Briefs, Pages 267-276

Pope S.B. (1975): A more general eddy-viscosity hypothesis. J. Fluid Mech. Vol. 72; Pages 331-340

Speziale C.G., Sarkar S., and Gatski T.B. (1991): Modelling the Pressure-Strain Correlation of Turbulence: An Invariant Dynamical Systems Approach. J. Fluid Mech., Vol. 227 Pages 245-272